Orientational Changes of Troponin C Associated with Thin Filament Activation†

Hui-Chun Li and Piotr G. Fajer*

Institute of Molecular Biophysics and Department of Biological Science, Florida State University, Tallahassee, Florida 32306

Received July 18, 1994; Revised Manuscript Received September 12, 1994®

ABSTRACT: We have used electron paramagnetic resonance to describe the orientational changes of troponin C (TnC) accompanying muscle activation by Ca^{2+}. Rabbit skeletal TnC was labeled with maleimide spin label (MSL) at Cys-98 and reconstituted into an oriented skinned muscle fiber. About 70% of endogenous troponin C was replaced with labeled TnC, with a concomitant recovery of 80−90% of muscle tension. The nanosecond domain mobility present in solution, as determined from the EPR spectra of randomized samples, is fully inhibited in the reconstituted fibers. The orientational analysis revealed a bimodal orientational distribution of TnC in the absence Ca^{2+} and attached myosin heads. One of the components is well-ordered with its probe axis inclined at 22° to the fiber axis, while the other is more disordered and inclined at 58°. Ca^{2+} and/or cross-bridge binding significantly disordered the labeled domain and increased the average probe axis angle by 20−30° away from the fiber axis. The order for the magnitude of angular tilt was Ca^{2+} < myosin cross-bridges < Ca^{2+} and cross-bridges. Thus, TnC exists in many different orientational conformations depending on which ligand is bound. We believe that these conformations reflect different activation mechanisms by Ca^{2+} and cross-bridge binding.

The thin filament of vertebrate striated muscle is composed of actin, tropomyosin, and troponin (Tn). Troponin is a complex of three proteins: troponin C (TnC),[1] the Ca^{2+} binding component; troponin T (TnT), the tropomyosin binding subunit; and troponin I (TnI), the inhibitory subunit capable of binding to actin and inhibiting actomyosin ATPase activity. Calcium released on neural stimulation from the sarcoplasmic reticulum binds to TnC, triggering a sequence of events that ultimately give rise to muscle contraction. According to the "steric blocking model" in the relaxed (Ca^{2+}-free) state of muscle, tropomyosin assumes a position on the actin filament in which it effectively blocks the attachment of myosin cross-bridges to actin. On activation, tropomyosin moves to clear the myosin−actin interaction site, thereby permitting cross-bridge cycling and contraction of the muscle (Haselgrove, 1972; Huxley, 1972; Parry & Squire, 1972). This model has been modified since its inception to allow for the regulatory role of attaching myosin heads as well as for the Ca^{2+} regulation of the steps subsequent to binding (Chalovich et al., 1981; Chalovich & Einsenberg, 1982; Geeves, 1991; Zou & Phillips, 1994).

Irrespective of the details of tropomyosin's role, it is clear that conformational changes are initiated on troponin C and then propagated via changes in the protein−protein interactions of troponin, tropomyosin, and actin. On the basis of the atomic structure of TnC, Herzberg and colleagues (1986) proposed a molecular model for this initial conformational change in TnC. The relative disposition of the helical segments in the Ca^{2+}-free N-terminal domain of crystalline TnC is more compact than those in the Ca^{2+}-filled C-terminal domain of TnC. The movement of the B/C pair of helices away from the A/D pair on Ca^{2+} binding exposes a patch of hydrophobic residues on TnC, providing a binding site for another troponin subunit (TnI). Changes of distance between labeled sites on TnC lent strong support for such a model [reviewed in Grabarek et al. (1992)]. There is however strong evidence that TnC exists in multiple configurations when complexed with other regulatory proteins as reflected in the distribution of distances and fluorescence yield (Zot & Potter, 1989; Wang et al., 1993).

The recent development of methods for TnC extraction from and reconstitution into fibers (Moss, 1992) has made it possible to follow the conformational changes of TnC in skinned fiber systems. In this study, we characterize these changes in terms of the orientational distribution of troponin C labeled at Cys-98 with a maleimide spin label (MSL). Taking advantage of the high orientational sensitivity of electron paramagnetic resonance (EPR) (Thomas & Cooke, 1980; Fajer, 1994a), we have determined that troponin C flexibility is significantly inhibited when reconstituted in fibers and that the conformations of TnC are different depending upon whether Ca^{2+} or myosin heads are bound.

MATERIALS AND METHODS

Sample Preparation. New Zealand White rabbits were sacrificed by CO_2 asphyxiation and bled, and small strips of psoas muscle (~2 mm diameter) were removed at room temperature. The fiber bundles were incubated on a shaker in fiber glycerinating solution (FG) for 24 h and then transferred to fiber storage (FS) solution for 48 h, prior to ultimate storage at −20 °C. Composition of all solutions is listed in Table 1. Fibers were stored for a maximum of 3 months.

† Research was sponsored by National Science Foundation Grant IBN-9206658 and by an Initial Investigator Award of the American Heart Association (to P.F.).

* To whom correspondence should be addressed; e-mail address: Fajer@sb.fsu.edu.

® Abstract published in *Advance ACS Abstracts,* October 15, 1994.

[1] Abbreviations: ATP, adenosine 5′-triphosphate; DITC, diisothiocyanate; EDTA, ethylenediaminetetraacetic acid; EGTA, ethylene glycol bis(β-aminoethyl ether)-*N,N,N′,N′*-tetraacetic acid; MOPS, 3-(*N*-morpholino)propanesulfonic acid; MSL, *N*-(1-oxy-2,2,5,5-tetramethyl-4-piperidinyl)maleimide; EPR, electron paramagnetic resonance; ST-EPR, saturation transfer electron paramagnetic resonance; S1, myosin subfragment 1; TFP, trifluoperazine; TnC, troponin C; TnI, troponin I; TnT, troponin T.

0006-2960/94/0433-14324$04.50/0

Table 1: Solutions[a]

	KAc (mM)	KPr (mM)	$MgCl_2$ (mM)	EGTA (mM)	MOPS (mM)	ATP (mM)	$CaCl_2$ (mM)	glycerol (%)	NaN_3 (mM)	EDTA (mM)	TFP (mM)	triton (%)
FG	60		2	10	25			25	1			0.5
FS	60		2	1	25			50	1			
rigor		130	2	1	20				1			
relaxation (ATP)		130	7	1	20	5			1			
contraction (ATP + Ca^{2+})		130	7	1	20	5	1.5		1			
TnC extraction					10					5	0.5	
TnC reconstitution		130	7	1	20	5			1			

[a] All solutions were adjusted to pH 7.0 at 4 °C.

TnC was purified according to the method of Potter (1982) with the following modifications: 0.1 mM PMSF was added to the ether powder preparation to prevent proteolysis. The DTT concentration was increased to 2 mM during the extraction of TnC from the crude troponin complex. The crude troponin extract was concentrated to less than 30 mL with an Amicon ultrafiltration cell (Model 202, Amicon Corp., Lexington, MA) with a YM 30 membrane. The sample was then dialyzed against urea buffer (6 M urea, 25 mM Tris, 1 mM EDTA, and 2 mM DTT, pH 8). The 8 M urea stock solution was first deionized by passing it through an ion-exchange column packed with a mixed bed resin (AG 501-X8D, Bio-Rad Laboratory, Hercules, CA).

Cys-98 in TnC was labeled with *N*-(1-oxy-2,2,6,6-tetramethyl-4-piperidinyl)maleimide (MSL, Aldrich Chemical Co., Milwaukee, WI) following the protocol of Wang and Gergely (1986). Samples of approximately 25 μM TnC in 20 mM HEPES, 0.1 M KCl, and 2 mM EDTA, pH 7.5, were first pretreated with 10 mM DTT for 2−3 h and then incubated with a 3-fold excess of MSL for 4 h at 20 °C. The extent of labeling was determined by calculating the spin label concentration from the second integral of the EPR signal intensity, and protein concentration was measured from the absorbance at 280 nm ($\epsilon_{280} = 0.18\ M^{-1}\ cm^{-1}$).

Spin-labeled TnC in the presence or absence of Ca^{2+} (2.4 mM) was cross-linked to preactivated diisothiocyanate (DITC) glass beads (Sigma Chemical Co, St. Louis, MO), at an equimolar ratio of protein and isothiocyanate.

TnC extraction was accomplished essentially according to Moss (1992). Thin fiber bundles (10−20 single fibers) were prepared from glycerinated rabbit psoas muscle. For fiber EPR experiments, endogenous TnC was extracted overnight with 5 mM EDTA, 10 mM MOPS, and 500 μM TFP (trifluoperazine), pH 7.0, at 4 °C. The extent of extraction was quantified by gel electrophoresis and assayed functionally by measuring the loss of active tension. Fibers depleted of endogenous TnC were incubated with MSL−TnC (~12 μM) in relaxing solution (see Table 1) overnight at 4 °C. The extent of reconstitution was assayed quantitatively by both gel electrophoresis and by the increase of active tension. For fiber mechanics, TnC was extracted for 15 min and reconstituted for 40 min since smaller bundles (3~5 single fibers) were used.

Ghost fibers were prepared by incubation of TnC-depleted fiber bundles with Hasselbach−Schneider solution (10 mM MOPS, 1 mM EGTA, 600 mM KCl, 0.5% Triton, and 5 mM Mg-ATP, pH 7.0) for 30 min to depolymerize the intrinsic myosin.

SDS−PAGE. A total of 2−5 mg of muscle fibers was dissolved in 20−50 μL of sample buffer (62.5 mM Tris, 1% SDS, 20 mM DTT, 2 mM EDTA, 40% glycerol, and 0.01% bromophenol blue), dispersed for 15−30 min in a sonicator (Mettler ME 1.5), and heated at 100 °C for 2 min. Samples were then applied to 8 × 10 mm SDS minigels (Hoeffer SE-250 Mighty Small II). The acrylamide/*N*,*N*′-methylenebisacrylamide ratio was 29:1, with a final 12% concentration of acrylamide in the separating gel and 9% in the stacking gel. The pH of the separating gel was increased to 9.3 (Giulian et al., 1983). The electrode buffer consisted of 0.025 M Tris, 0.192 M glycine, and 0.1% SDS, pH 8.5. Gel electrophoresis was performed at a constant voltage of 100 V for ~2.5 h at room temperature. Coomassie Brilliant Blue R250 stained gels were scanned with an 8-bit page scanner (ScanMaker II, Microtek Lab, Torrance, CA). The gel image was transformed into a density profile using Global Lab software (Data Translation, Marlboro, MA). The profile was then analyzed with a Simplex optimization routine developed in our laboratory, which fitted up to five Gaussian peaks to resolve overlapping bands.

Muscle Mechanics. Three to five single fibers (10 mm long) were attached to a force transducer (Model 400A, Cambridge Technology, Cambridge, MA) and a length controller (Model 602X, Cambridge Technology). The extraction and reconstitution with TnC was accomplished directly in the tensiometer well to avoid variability between the preparations. Active tension was normalized to the cross sectional area of the fibers as determined under a dissecting microscope (Nikon 2B). All measurements were performed at 23 °C.

Electron Paramagnetic Resonance. Reconstituted fibers (0.5 mm, consisting of 4−5 thin fiber bundles) were placed in 1-mm glass capillaries and held isometrically by surgical silk thread (no. 6; Deknatel, Fall River, MA) that was tied to the ends of the bundle. Solutions were continuously flowed over the fibers at a rate of 0.2 mL/min, controlled by a peristaltic pump (P3, Pharmacia, Piscataway, NJ). EPR experiments were performed on a Bruker ECS-106 spectrometer (Bruker Inc., Billerica, MA), using a TM_{110} cavity modified to accept samples parallel to the static magnetic field or in a TE_{102} cavity with the fiber axis perpendicular to the magnetic field for ST-EPR spectra. Conventional EPR spectra were recorded at a microwave power of 0.144 G microwave field and a modulation field of 2.5 G, while the ST-EPR spectra were obtained at saturating fields of 0.25 G and a modulation amplitude of 5 G. Spectra were acquired, averaged, and analyzed using an IBM-compatible personal computer with spectral analysis software developed in our laboratory.

Spectral Simulations. EPR simulations are described in Fajer (1994a,b). Briefly, the spectral fitting was achieved by utilization of a Simplex routine. Myofibrilar spectra were simulated with a modified algorithm of Siderer and Luz

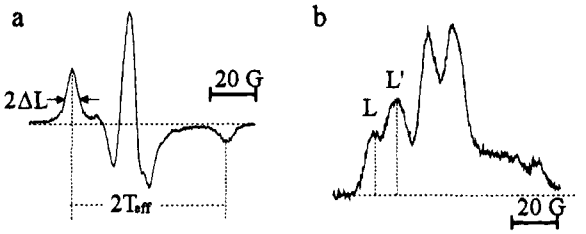

FIGURE 1: EPR spectrum of MSL−TnC immobilized on DITC glass beads: (a) conventional EPR and (b) ST-EPR.

(1980) in order to obtain magnetic tensors and intrinsic line width parameters. The fiber spectra were simulated using an Eulerian angles formalism, in which the orientational distribution is defined by the angle of the probe's principal tensor axis (z), the fiber axis (β), and the rotation about the z-axis of the probe (α). The probe disorder was modeled as Gaussian, with a half width of $\Delta\beta$ and $\Delta\alpha$. In order to limit computational time for the broad spectra, the step size was 5° on β, 45° on α, and 10° on $\Delta\alpha$ and $\Delta\beta$. The large step size on α is justified by the relatively small sensitivity of the EPR spectra to wide angular distributions. Powder simulations were carried out on a Cray-YMP computer, and the oriented spectra were simulated on a 50-MHz PC.

RESULTS

Solution Studies

Spin Label Immobilization. A prerequisite for all orientational studies using extrinsic labels is the rigidity of the probe with respect to the protein surface. The standard approach used to detect librational motion of a label is to immobilize the protein and observe the probe's mobility in the nanosecond range using conventional EPR and in the microsecond to millisecond range with ST-EPR. TnC was cross-linked to DITC beads, and the two spectra obtained and shown in Figure 1 are characteristic of the rigid limit on both time scales. The splitting between the outer extremes ($2T_{eff}$, effective splitting) of the spectrum is 68.4 G, comparable to the rigid limit for MSL bound to many other proteins, e.g., 68.5 G for MSL−actin (Thomas et al., 1979), 68.5 G for MSL−tropomyosin (Szczesna & Fajer, unpublished), 68.0 G for MSL labeled Ca^{2+}-ATPase (Hidalgo et al., 1976), and 69.0 G for MSL−hemoglobin (Johnson, 1981). The absence of librational motion is further confirmed by the saturation transfer EPR line height ratios L'/L = 1.6 (Figure 1b), which are at the rigid limit of the ST-EPR method (Thomas et al., 1976). Since the rigid limit for conventional EPR is 0.1 μs and for ST-EPR is 1−3 ms, we are confident that the spin probe is rigidly attached to the protein and will faithfully report the orientation of troponin C.

Equally important is to ascertain that no librational motion is introduced by Ca^{2+} binding to the regulatory sites of TnC. The binding of ligands has been known to induce local mobility of spin labels (Barnett & Thomas, 1987). As shown in Table 2, within experimental error Ca^{2+} did not reduce the splitting or the peak height ratio of the ST-EPR spectra.

Mobility of MSL−TnC. The mobility of the labeled troponin C was investigated by conventional EPR. Modulation of the signal anisotropy is directly related to the nanosecond mobility of the label. As seen in Figure 2, the powder-like signal of the immobilized TnC becomes motionally narrowed for troponin C in solution, giving rise to three sharp peaks with $2T_{eff}$ = 36.9 ± 0.1 G. The rotational correlation time, τ_r is estimated by the relationship

$$\tau_r = a(1 - T_{eff}/T_{max})^b$$

where T_{max} is defined as the rigid limit for the particular spin label, $a = 5.4 \times 10^{-10}$ s, and $b = -1.36$ for Brownian motion (Freed, 1976). The calculated τ_r for MSL−TnC in solution is 1.6 ns, assuming $2T_{max}$ is 68.4 G from MSL−TnC immobilized on DITC beads (Figure 1a). This motion is too slow to be either free librational rotation of the label or the rotation of the C−S bond of the cysteine (τ_r = 0.1−0.5 ns; Oton et al., 1981) but too fast to represent tumbling of the whole protein. A spherical molecule of equivalent molecular weight and hydration of 0.2 g of water/g of

Table 2: Calcium Effect on Immobilized MSL−TnC

MSL−TnC/DITC beads[a]	$2T_{eff}$ (EPR) (G)	L'/L (ST-EPR)
+EDTA	68.4 ± 0.2	1.6 ± 0.1
+Ca^{2+}	68.8 ± 0.1	1.5 ± 0.1

[a] MSL−TnC with 2 mM EDTA or 2.4 mM $CaCl_2$ in the buffer was cross-linked to DITC glass beads as described in Materials and Methods.

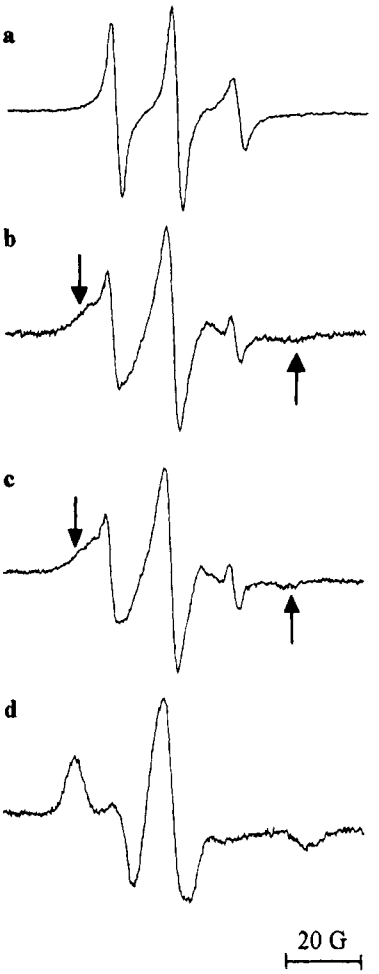

FIGURE 2: EPR spectrum of MSL−TnC (a) in EDTA, (b) with 2.4 mM $CaCl_2$ in solution, (c) with 2.4 mM $MgCl_2$ in solution, and (d) with reconstituted myofibrils. Arrows indicate the slow tumbling species in the presence of Mg^{2+} or Ca^{2+}.

protein is expected to tumble with $\tau_r = 7$ ns (Cantor & Schimmel, 1980). Even if TnC is assumed to have an extended conformation as observed in the crystal, the rotational correlation time should be the harmonic mean of the correlation times for rotation about the short (τ_b) and long axis (τ_a) of a prolate ellipsoid with an axial ratio of 3:1. Using Perrin's equations (Cantor & Schimmel, 1980), $\tau_a = 0.8\tau_0$ and $\tau_b = 1.14\tau_0$, where τ_0 is the correlation time for an equivalent sphere (7 ns). The shortest calculated correlation time (5.6 ns) is significantly larger than the correlation time observed here; hence, spin label motion must reflect domain motion of the helix containing Cys-98.

The addition of Mg^{2+} or Ca^{2+} reduces the mobility of TnC as indicated by the appearance of a larger splitting than that of the apoprotein (52 ± 0.1 G vs 36.9 ± 0.1 G, see arrows in Figure 2b,c). The slow tumbling species ($\tau_r = 3.8$ ns, using 52 G as $2T_{eff}$) accounts for 75% of the total intensity as estimated by spectral subtraction of apoprotein and Mg^{2+}-TnC/Ca^{2+}-TnC. The remaining 25% of the signal intensity represents a fast tumbling species that does not respond to the binding of Ca^{2+} and may represent a different label environment. A similar decrease of probe mobility was observed previously for spin-labeled TnC (Ohnishi et al., 1975; Potter et al., 1976) and also for TnC labeled with a fluorescent probe (Wang, C. K., et al., 1992). Most likely, the binding of divalent ions to sites III and IV results in a conformational change limiting the motional freedom of Cys-98, consistent with a large change in α helical content (Kay et al., 1987). Saturation of the regulatory sites I and II with Ca^{2+} has a much smaller effect on the domain mobility and overall protein structure.

The incorporation of TnC into myofibrils inhibits totally its nanosecond mobility. The spectral line shape of the reconstituted MSL−TnC myofibrils (Figure 2d) is very similar to that of the rigid limit of TnC (Figure 1a), with a separation of the outermost peaks of 66.0 ± 0.5 G. This implies a strong interaction of TnC with other regulatory proteins inducing protein immobilization. The lower bound for the correlation time within myofibrils is 0.1 μs, which is the limit of motional sensitivity of conventional EPR.

Studies of Reconstituted Fibers

Endogenous TnC Extraction and MSL−TnC Reconstitution. The stoichiometry of TnC extraction and reconstitution was determined by quantitative gel electrophoresis (Figure 3). The area under the peaks was used to evaluate the amount of protein in the fiber. A linear relationship between TnC load and peak area has been established (data not shown). Since the sample loading on each lane may differ, TnC was normalized to the total TnI and LC1 content, which are not extracted under these conditions (Moss et al., 1985). On average, 70% of the total TnC was extracted, and incubation with MSL−TnC recovered 95% of the original TnC concentration (Table 3).

Since the protein stoichiometry does not distinguish whether the reconstitution is functional or not, the mechanical performance of the fibers was evaluated (Figure 4). After extraction of endogenous TnC, only 0−40% of the Ca^{2+}-induced control tension remained, as noted previously by Moss et al. (1985). Upon reconstitution, 80−95% of the

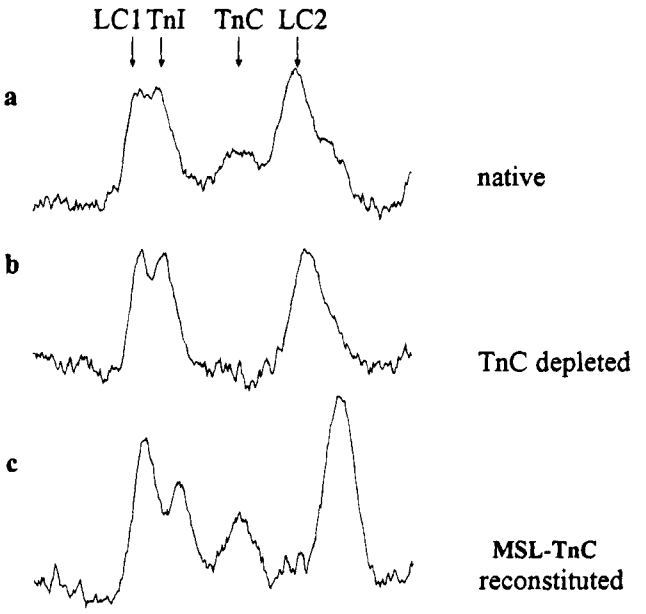

FIGURE 3: Intensity profile of Coomassie Blue-stained SDS−PAGE gel: (a) control fibers; (b) TnC-extracted fibers; and (c) MSL−TnC-reconstituted fibers.

Table 3: Extent of TnC Extraction and Reconstitution

sample	TnC content (SDS gel) (%)	active tension ($n = 3$) (%)
control	100	100
TnC-extracted	36% ± 5	10% ± 8
MSL−TnC reconstituted	95% ± 5	80% ± 15

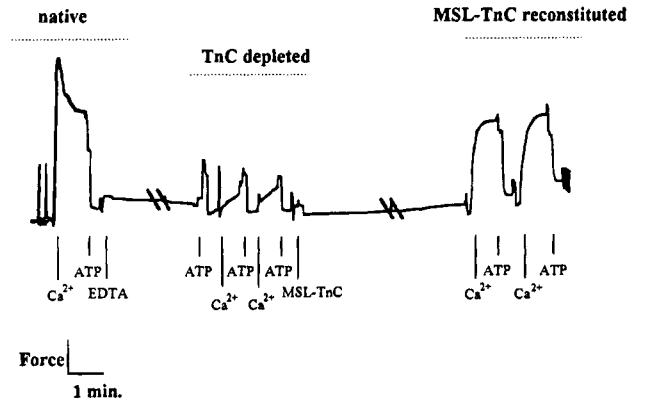

FIGURE 4: Tension trace of a bundle of three muscle fibers during TnC extraction and reconstitution with MSL−TnC. Ca^{2+}, contraction; ATP, relaxation; EDTA, TnC extraction; MSL−TnC, MSL−TnC reconstitution. The trace was interrupted for 20 and 40 min during extraction and reconstitution, respectively. The composition of the extraction and reconstitution solutions are given in Table 1.

control active tension was restored (Table 3). The resting tension (tension developed in relaxation) remained at approximately the same level as before TnC extraction, indicating that no other troponin subunits (e.g., TnI) were damaged during extraction and reconstitution. Thus, endogenous TnC can be replaced with labeled TnC and the labeling and reconstitution does not perturb the function of the troponin complex.

Orientation of TnC in Fibers. Conventional EPR spectra of fibers oriented parallel to the magnetic field are particularly sensitive to the spin label distribution around the fiber axis. A comparison of the spectrum of the relaxed fibers (Figure 5a) with that of TnC on the glass beads (Figure 1a),

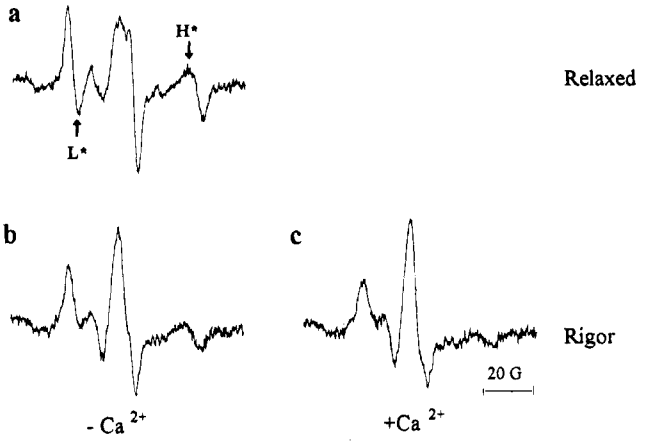

FIGURE 5: EPR spectra of MSL−TnC reconstituted into fibers: (a) relaxed state; (b) rigor state; and (c) rigor state with 2 mM $CaCl_2$.

or randomly distributed myofibrils (Figure 2d), reveals significant order in the relaxed fibers. The distribution of the intensity below the baseline for the low-field trough (L* in Figure 5a) and the positive high-field peak (H*, in Figure 5a) are qualitative fingerprints of nonrandom orientational distribution. For the isotropically distributed spins of TnC in the myofibrils (Figure 2d) or TnC on the glass beads (Figure 1a), the low-field resonance has a positive amplitude, while the high-field is always negative. When the probe orientational distribution is modeled as a Gaussian, the above features appear only when the label's disorder is larger than ±90° for the angle of the major axis of the label with respect to the fiber axis (Fajer, 1994b). Another feature is the splitting of 69.6 ± 0.2 G for the relaxed fiber as compared to 68.4 ± 0.2 G for the TnC on the glass beads. Since the spectral extremes arise from the resonance of spins whose axes are aligned with the direction of the magnetic field, the large splitting in the spectrum from the relaxed fibers indicates that a significant fraction of the spin labels are parallel to the magnetic field. Furthermore, the widths of the low- and high-field resonances are considerably smaller (e.g., 2.2 ± 0.1 G in the low-field peak in the relaxed fibers, see Figure 5a, as compared to 3.2 ± 0.1 G in myofibrils), also implying ordering of the probes.

Orientational Change Induced by Cross-Bridge Attachment. The binding of myosin heads to the thin filament greatly perturbs the distribution of TnC (Figure 5b). The average angle of this distribution is larger than in the relaxed fibers (Figure 5a) since the effective splitting is 0.8 G smaller than that in the relaxed specta (Table 4). This change of the average orientation is accompanied by increased disorder because the width of the low-field peak increases on cross-bridge attachment (from 2.2 ± 0.1 G to 2.6 ± 0.1 G; Figure 5 and Table 4). However, a close inspection of the spectrum in the high-field region reveals a small positive H*, implying a residual order of the spin labels.

Orientation Change Induced by Calcium Binding to TnC. In the presence of the rigor cross-bridges, the addition of Ca^{2+} resulted in further disordering of MSL−TnC (Figure 5c). The absence of the positive H* peak implied that the labeled TnC was very disordered when Ca^{2+} bound to sites I and II; both of these sites are fully saturated at 1 mM free calcium. In the reconstituted fiber experiments, the non-specific sites III and IV in the C-domain are saturated with Mg^{2+} in relaxed and rigor fibers. In the presence of such large disorder, it is impossible to make a qualitative statement

Table 4: Spectral Parameters

sample	$2T_{eff}$[a] (G)	ΔL[b] (G)
	Solutions	
MSL−TnC	39.6 ± 0.1	
MSL−TnC + Mg^{2+}	52.1 ± 0.1	
MSL−TnC + Ca^{2+}	52.1 ± 0.1	
myofibrils	66.0 ± 0.5	3.2 ± 0.1
	Fibers	
relaxed	69.6 ± 0.2	2.2 ± 0.2
rigor	68.8 ± 0.2	2.7 ± 0.2
rigor + Ca^{2+}	67.6 ± 0.2	3.5 ± 0.2
	Ghost Fibers	
ghost fibers	68.9 ± 0.2	2.1 ± 02
ghost + S1	67.3 ± 0.2	2.9 ± 0.2
ghost + Ca^{2+}	67.5 ± 0.2	2.6 ± 0.2
ghost + S1 + Ca^{2+}	66.8 ± 0.2	3.6 ± 0.2

[a] $2T_{eff}$, the separation between the outermost peaks. [b] ΔL, half-width at half-height of low-field peak.

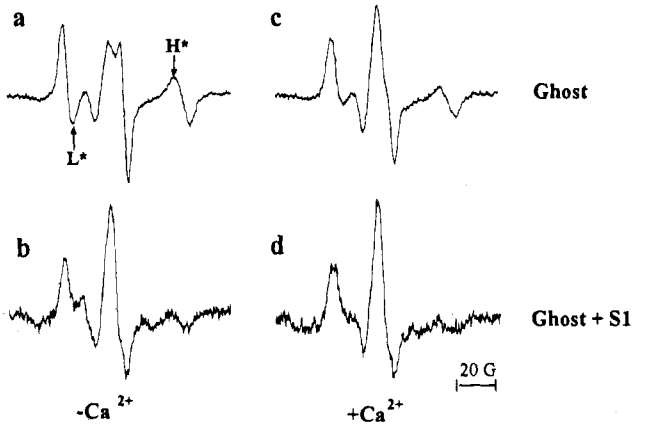

FIGURE 6: EPR spectra of MSL−TnC in (a) myosin-extracted ghost fiber; (b) ghost fiber decorated with S1; (c) ghost fiber with calcium; and (d) ghost fiber decorated with S1 in the presence of calcium.

about the average angle. The addition of Ca^{2+} when the fiber is relaxed would initiate fiber contraction, and the effect of Ca^{2+} on TnC would be complicated by the attachment of the myosin heads.

Orientation of TnC in Ghost Fibers. In order to investigate the effect of Ca^{2+} in the absence of myosin cross-bridges, we have removed myosin from the fiber lattice by dissolving the thick filaments in high ionic strength solution (Hasselbach−Schneider solution). The myosin-extracted ghost fibers provide a convenient model to monitor directly the Ca^{2+} effect on TnC in the thin filaments, without the complication of cross-bridge attachment.

The addition of 1 mM free Ca^{2+} to ghost fibers results in disordering of TnC (compare Figure 6a and 6c), reflected in the increase of the low-field peak width, 2.1 ± 0.1 G and 2.6 ± 0.1 G in the absence and presence of Ca^{2+}, respectively. The disorder is not isotropic as implied by the trough (L*) in the low-field region as well as by the peak (H*) at the high-field region.

When isolated myosin heads (S1) are infused into ghost fibers, TnC becomes disordered in a manner similar to that observed in the fibers upon removal of ATP, with subsequent rigor cross-bridge formation (compare Figure 5b and Figure 6b). As in the skinned fibers, calcium and myosin heads have a synergistic effect on TnC, resulting in a spectrum that closely resembles that of randomized myofibrils. The observed changes were fully reversible; the disordering of

Table 5: Magnetic Tensors and Line Width Parameters[a]

parameter	value
g_x	2.01084 ± 0.00009
g_y	2.00855 ± 0.00005
g_z	2.00510 ± 0.00004
T_x	8.3 ± 0.3
T_y	9.3 ± 0.5
T_z	34.4 ± 0.1
Γ_L	2.7 ± 0.1
Γ_G	2.4 ± 0.1
Γ_{mG}	0.7 ± 0.1

[a] g denotes the g tensor, and T denotes the hyperfine tensor (in G). Γ_L and Γ_G are orientationally independent Lorentzian and Gaussian line widths (in G) (Fajer et al., 1990). Γ_{mG} is the manifold-dependent Gaussian. Line widths are reported as half-width at half-maximum height. Errors are the standard deviations of seven searches.

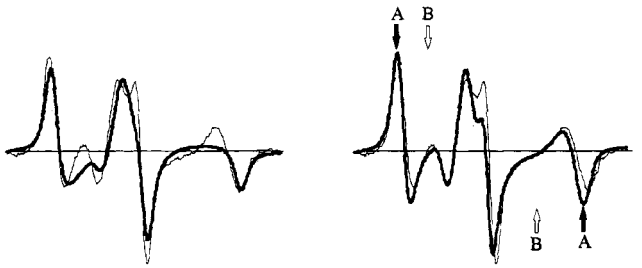

FIGURE 7: Computer simulations of the TnC reconstituted ghost fibers (thick line) and experimental spectra (Figure 6a) (thin line): (a) best single-component simulations; (b) bimodal distribution, component A (22° ± 14°, 90° ± 20°), solid arrows; component B (58° ± 27°, 30° ± 0°), open arrows, mixed in a ratio of 49:51 mol %.

TnC is reversed by removal of Ca^{2+} with EGTA or by S1 dissociation from ghost fibers on the addition of ATP.

Spectral Simulations

Determination of Angle-Independent Spectral Parameters. The accurate determination of the magnetic tensor values and line width parameters is a prerequisite for the high-resolution determination of the angular distribution from oriented spectra (spectra obtained from ordered samples). The tensor and line width values are determined by analyzing the spectrum of a randomly oriented sample, e.g., the myofibrils (Figure 2d). The tensors and line width values determined by Simplex fitting of the data in Figure 6 are shown in Table 5.

Bimodal Orientational Distribution. The quantitative analysis confirms qualitative statements made above about the distribution of the TnC, but in the case of relaxed fibers it yielded an unexpected result. The spectrum (Figure 6a) was first simulated by assuming a single orientational population with Gaussian distributions of width $\Delta\alpha$, $\Delta\beta$ centered about α_0 and β_0. The values of the four orientational parameters were not constrained; each was allowed to vary between 0 and 90°. However, even the best simulated spectrum (Figure 7a) did not reproduce the spectral features such as the low-field negative excursion (L*) and the high-field positive H* peak.

The goodness of fit (χ^2) value improved 5−10-fold over the single-component fit when a linear combination of two spectra was assumed (Figure 7b). The two spectral components are assumed to have the same magnetic tensors and line widths but different angular distributions. The two distributions that were identified are ~49 mol % of component A, with an average angle (β) at 22°, and component B which makes up the remaining ~51 mol %, with an average angle at 58° with respect to the fiber axis. The origin of the two orientational components is not clear, but most likely it represents two orientational isomers of Cys-98, which have been observed in the crystal structure of TnC (Herzberg & James, 1988; Satyshur et al., 1994). The two components display a different degree of order with respect to the fiber axis, component A has an axial Gaussian width ($\Delta\beta$) of ±14°, while the component B width is ±27°. The difference in the width of distribution is unlikely to be the result of different orientations of the probe with respect to the protein, but we will be able to address this when the orientation of the probe with respect to the protein is determined. Such a study is currently underway. The large disorder of one of the components cannot be attributed to disordering of the thin filament since labeled myosin heads decorating such fibers display a narrow angular distribution of ±8° (Fajer, 1994b).

Table 6: Angular Distribution of Component A in Ghost Fiber Experiments[a]

sample	β_0 (deg)	$\Delta\beta$ (deg)	fraction
ghost	22 ± 5	14 ± 5	0.49 ± 0.05
ghost + Ca^{2+}	45 ± 5	45 ± 5	0.9 ± 0.1
ghost + S1	55 ± 5	45 ± 5	0.9 ± 0.1
ghost + S1 + Ca^{2+}	60 ± 5	45 ± 5	0.9 ± 0.1

[a] β_0, the average tilt angle of the probe with respect to the fiber axis. $\Delta\beta$, the half-width of Gaussian distribution centered about β_0. Data are obtained from simulating the spectra in Figure 6 with bimodal (Figure 7b) Gaussian orientational distribution. Only one axial tilt angle of probe axis to the fiber axis (β) is reported. The azimuthal angle (α) is less well-defined and was omitted.

The data in Figure 6b−d were similarly analyzed with the bimodal orientational distribution, and the results are listed in Table 6. The addition of Ca^{2+} increases the average tilt (β) by 21°, with a parallel increase of the disorder ($\Delta\beta$) about the average angle (from 14° to 45°). Interestingly, the change in the disorder is of a similar magnitude as the change in the tilt angle, cautioning against the interpretation of spectroscopic signals that do not resolve between the average angle and the distribution about that angle (fluorescence anisotropy, linear birefringence) in terms of changes in either of the orientational parameters alone. Induced disorder obscures the resolution of the second component; 90% of the spectrum is accounted for by a single component (Table 6). Equally, the resolution of the second polar angle α is limited by a broad component due to the smaller anisotropy of the probe x- and y-axes (Fajer, 1994b); therefore, in the subsequent discussion we will consider only the axial tilt of the z-axis of the probe with respect to the fiber axis.

The orientational change on myosin head binding is different from that produced by the binding of Ca^{2+} to TnC. The change of the tilt angle is more pronounced, $\beta_0 = 55°$, i.e., the binding of the heads reorients the Cys-98 domain by 33° with respect to the fiber axis. There is also a noticeable increase of domain disorder similar to that produced by Ca^{2+} binding (see Table 6). As noted earlier, the effect of Ca^{2+} and S1 is synergistic, the infusion of S1 to Ca^{2+} ghosts increases the tilt angle by a further 15°.

DISCUSSION

Summary of Results. Our study provides direct evidence that in functionally reconstituted muscle fibers TnC exists

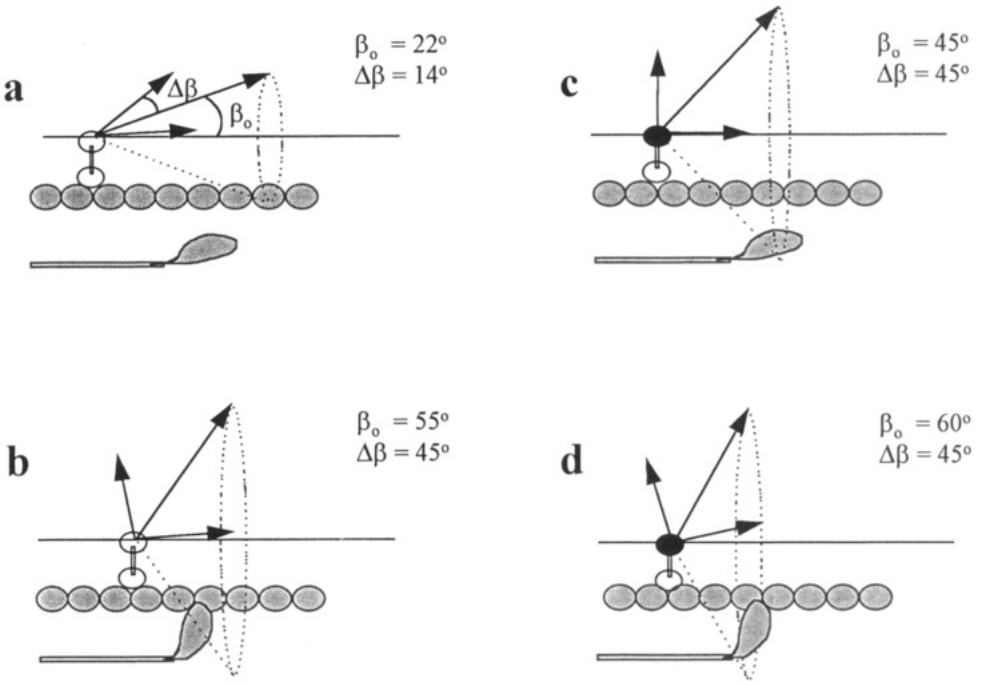

FIGURE 8: Illustration of possible conformations of TnC in muscle fibers. This figure shows the reversible structural changes of TnC as detected by EPR spectral changes under (a) relaxation; (b) rigor; (c) with bound Ca^{2+} in the absence of rigor cross-bridges; and (d) with bound Ca^{2+} in the presence of rigor cross-bridges. The arrows denote the orientation of the spin label with respect to the fiber.

in a number of different orientational conformations. Orientational distributions of these conformations are distinct depending on the presence of Ca^{2+} and/or attached cross-bridges. The relationships between the various conformational states studied here is shown in Figure 8. In a, TnC has a narrow orientational distribution in relaxed fibers (only component A is shown here for simplicity); in b Ca^{2+} bound to the N-terminal domain of TnC induces a 23° rotation of the C-terminal domain, accompanied by the disordering of TnC; in c the binding of myosin heads in the absence of Ca^{2+} causes a somewhat larger 33° rotation of TnC; and in d the effect of Ca^{2+} and S1 are synergistic, producing a largest axial rotation of 38°. It seems that, at least as sensed by Cys-98, the structural aspects of activation by calcium are different than the mechanism of activation by the myosin heads. These findings are of particular importance because the effects are observed in the absence of the nanosecond flexibility of TnC, which has been implicated in the bending of the central helix to adopt in solution a compact conformation with the globular N- and C-domains in close proximity (Wang et al., 1993). This domain mobility is inhibited at least 30-fold, with correlation times outside the sensitivity of conventional EPR (>100 ns).

Relationship with Other Studies. A similar attempt to describe the structural change of TnC labeled with a fluorescence probe on Cys-98 was carried out by Gordon et al. (1988), who also concluded that myosin heads as well as Ca^{2+} have a disordering effect on TnC. However, due to the intrinsic limitation of the linear dichroism used in that study, the interpretation was ambiguous—the observed changes could be explained by either changes of orientation or disordering. EPR has the advantage of spectral resolution of orientations, with different orientations contributing to intensity at different field positions in the spectrum, which allows the determination of average angles as well as the width of distribution about that angle. It is possible to detect multiple orientational populations such as those shown here.

TnC reconstituted into fibers is well-ordered with respect to the fiber axis, and the orientational distribution is narrow. Spectral simulations suggest the presence of two populations in equal proportions; one with the probe axis at 22° with respect to the fiber axis, and the other more disordered with the probe at 58°. Since the reconstitution was stoichiometric and regulation of tension was restored, these populations cannot be artifacts of the reconstitution. The two populations probably do not correspond to overlap and nonoverlap regions of thin filaments since they are present in the ghost fibers. Naturally, we cannot exclude the possibility that the thin filament has a memory of actomyosin interactions and that structural differences in the two regions remain even after the removal of myosin and troponin C. Most likely though, the two orientations are due to orientational isomers of Cys-98 in TnC, as observed in crystals of both turkey and chicken TnC (Herzberg & James, 1988; Satyshur et al., 1994). Molecular modeling of MSL attached to Cys-98 did not reveal significant steric constraints imposed by the label on either of the isomers. However, the labeled domain is implicated in the interaction with TnI (Dalgarno et al., 1982; Leszyk et al., 1987, 1988), and these interactions might provide additional steric constraints on the orientation of the labeled cysteine in reconstituted complexes.

On the basis of the structure of TnC in crystals, particularly the difference of the C-terminal domain with bound divalent cation and the structure of the N-domain containing empty calcium binding sites, Herzberg, Moult, and James proposed a model according to which the binding of Ca^{2+} to sites I and II of TnC changes the interhelical angle, resulting in the movement of the B/C pair of helices away from the A/D pair (Herzberg et al., 1986). Such a movement opens a hydrophobic pocket in the N-domain, which might attract TnI, releasing the inhibition of actomyosin interactions. This model received strong support from the elegant work of Tao and associates, who using fluorescence energy transfer and various chemical cross-linkers showed a decreased distance

between parts of troponin C and I (including Cys-98) and a parallel increase of distance between TnI and actin (Tao et al., 1989, 1990; Park et al., 1994). Limiting the proposed opening of the interhelical angles by salt or disulfide bridges resulted in the impaired Ca^{2+} regulation of actomyosin interactions (Fujimori et al., 1990; Grabarek et al., 1990). The data presented here originate from a single site on TnC and, thus, do not directly support or negate the above model. However, our data indicate that there are a number of conformations of TnC rather than just the two proposed by Herzberg et al. (1986). Furthermore, although our labeled site is nearer the C-domain than the N-domain, it is clear that Ca^{2+} binding to the N-domain induces changes propagating all the way to the labeled site.

The binding of Ca^{2+} to the regulatory sites induced a significant rotation of the TnC, accompanied by large disordering ($\Delta\beta = 45°$). The increased width of the orientational distribution cannot be ascribed to disordering of the thin filament because the myosin heads bound to actin filaments display a very narrow angular distribution, $\Delta\beta = \pm 8°$ (Thomas & Cooke, 1980; Fajer, 1994b), which does not change on the addition of Ca^{2+}. This induced disorder might be related to the range of distances between TnI and TnC implied by the recent cross-linking studies of Park et al. (1994), but it might also represent the disorder of the complex. At this stage, we cannot say whether the disorder is dynamic, implying that troponin C is flexible, or whether it represents a range of static conformations of the protein. The effects of Ca^{2+} binding to distant regulatory sites is known to affect sulfhydryl reactivity, spin label mobility, and fluorescence of the extrinsic probe, even in the presence of complexed TnI and TnT (Onishi et al., 1975; Potter et al., 1976). As noted by these authors, all changes could be ascribed to the variation in the immediate environment since the accessibility of Cys-98 to solvent determines sulfhydryl reactivity, the hydrophobicity defines fluorescence yield, and the steric restrictions limit label mobility. Whether similar changes take place within the fiber is uncertain. As argued above, protein flexibility is severely limited, and the range of conformations observed in solution might be limited within fibers. Nevertheless, we can clearly observe interdomain communication between the N-terminal globular domain and the C-domain, postulated to be a part of the thin filament activation proces (Grabarek et al., 1986).

Although the attached myosin cross-bridges do not interact with TnC directly, we have observed a substantial orientational change induced by the myosin cross-bridges attachment to the thin filament in fibers. The myosin-induced change is not the same as that induced by calcium binding, differing mainly in the axial reorientation of the protein.

The involvement of myosin cross-bridges in thin filament regulation was first suggested by Bremel and Weber (1972) and explained by the models of Hill et al. (1980). Subsequent fluorescence studies using probes on Met-25 in the N-domain indicated changes in the probe environment induced by the cross-bridge attachment to the thin filament in skinned fibers (Kerrick & Hoar, 1987; Guth & Potter, 1987; Gordon et al., 1988; Zot & Potter, 1989; Morano & Ruegg, 1991). The fluorescence yield increase was larger than for Ca^{2+} binding and was dependent on the state of the cross-bridges, different for "weak", cycling, and rigor heads. These observations lead Zot and Potter (1989) to suggest that TnC is not a simple on−off switch, but that it may exist in a number of different conformations and that there is a reciprocal coupling between the binding of Ca^{2+} to TnC and the attachment of myosin cross-bridges to the actin filaments. The data presented here strongly support this conclusion, extend the distance of coupling to the E helix in the C-domain, and furthermore, identify the induced changes as the reorientation of the protein. We can speculate that the different conformations of TnC correspond to different states of the thin filament, as postulated by Geeves (1991): a "closed" state in the absence of myosin and Ca^{2+} binding in which the troponin C is well-ordered and the probe nearly parallel to the fiber axis; an "open" state allowing "weak" myosin binding, characterized by a more perpendicular orientation and large disorder; and an "activated" state with strongly bound myosin heads. More experiments, particularly during isometric contraction and low ionic strength relaxation, are clearly needed. Interestingly, the different states of TnC have their counterpart in tropomyosin. We have recently shown that in fibers reconstituted with MSL-labeled tropomyosin, the mobility was higher when the myosin heads were bound to the thin filaments (Szczesna & Fajer, 1994).

CONCLUSION

The observed EPR spectral changes provide direct evidence that TnC in skinned muscle fibers exists in a number of different orientational conformations: (a) in relaxed fibers, TnC has a narrow orientational distribution; (b) Ca^{2+} binding induces rotation and disordering of the labeled domain; and (c) cross-bridge binding results in a similar but larger rotation of this labeled domain. The orientational changes of TnC induced by Ca^{2+} binding and the cross-bridge attachment to actin filaments might provide a structural basis for the reciprocal coupling between myosin heads and Ca^{2+}, which leads to the high cooperativity of activation.

ACKNOWLEDGMENT

We thank Drs. Ken Taylor, Zenon Grabarek, and Terence Tao for helpful discussions and Elizabeth Fajer for help with the manuscript. We thank Dr. Tao for his gift of TnC used in preliminary studies.

REFERENCES

Barnett, V. A., & Thomas, D. D. (1987) *Biochemistry 26*, 314−23.

Bremel, R. D., & Weber, A. (1972) *Nature (New Biol.) 238*, 97−101.

Cantor, C. R., & Schimmel, P. R. (1980) *Biophysical Chemistry*, W. H. Freeman and Co., San Francisco.

Chalovich, J. M., & Eisenberg, E. (1982) *J. Biol. Chem. 257*, 2432−7.

Chalovich, J. M., Chock, P. B., & Eisenberg, E. (1981) *J. Biol. Chem. 256*, 575−8.

Dalgarno, D. C., Prince, H. P., Levine, B. A., & Trayer, I. P. (1982) *Biochim. Biophys. Acta 707*, 81−8.

Faber, R. J., & Fraenkel, G. K. (1967) *J. Chem. Phys. 47*, 2462−7.

Fajer, P. G. (1994a) *Proc. Natl. Acad. Sci. U.S.A. 91*, 937−41.

Fajer, P. G. (1994b) *Biophys. J. 66*, 2039−50.

Fajer, P. G., Bennett, R. L. H., Polnaszek, C. F., Fajer, E. A., & Thomas, D. D. (1990) *J. Magn. Reson. 88*, 115−25.

Freed, J. H. (1976) in *Spin Labeling. Theory and applications* (Berliner, L. J., Ed.) Vol. I, pp 53−132, Academic Press, Inc., New York.
Fujimori, K., Sorenson, M., Herzberg, O., Moult, J., & Reinach, F. C. (1990) *Nature 345*, 182−4.
Geeves, M. A. (1991) *Biochem. J. 274*, 1−14.
Giulian, G. G., Moss, R. L., & Greaser, M. (1983) *Anal. Biochem. 129*, 277−87.
Gordon, A. M., Ridgway, E. B., Yates, L. D., & Allen, T. (1988) *Adv. Exp. Med. Biol. 226*, 89−99.
Grabarek, Z., Leavis, P. C., & Gergely, J. (1986) *J. Biol. Chem. 261*, 608−13.
Grabarek, Z., Tan, R. Y., Wang, J., Tao, T., & Gergely, J. (1990) *Nature 345*, 132−5.
Grabarek, Z., Tao, T., & Gergely, J. (1992) *J. Muscle Res. Cell. Motil. 13*, 383−93.
Guth, K., & Potter, J. D. (1987) *J. Biol. Chem. 262*, 13627−35.
Haselgrove, J. C. (1972) *Cold Spring Harbor Symp. Quant. Biol. 37*, 341−52.
Herzberg, O., & James, M. N. G. (1988) *J. Mol. Biol. 203*, 761−79.
Herzberg, O., Moult, J., & James, N. G. (1986) *J. Biol. Chem. 261*, 2638−44.
Hidalgo, C., Thomas, D. D., & Ikemoto, N. (1978) *J. Biol. Chem. 253*, 6879−87.
Hill, T. L., Eisenberg, E., & Greene, L. (1980) *Proc. Natl. Acad. Sci. U.S.A. 77*, 3186−90.
Hoar, P. E., Mahoney, C. W., & Kerrick, G. L. (1987) *Pflugers. Arch. 410*, 30−6.
Huxley, H. E. (1972) *Cold Spring Harbor Symp. Quant. Biol. 37*, 361−76.
Johnson, M. E. (1981) *Biochemistry 20*, 3319−28.
Kay, C. M., Mccubbin, W. D., & Sykes, B. D. (1987) *Biopolymer 26*, S123−44.
Laemmli, U. K. (1970) *Nature (London) 227*, 680−5.
Leszyk, J., Collins, J. H., Leavis, P. C., & Tao, T. (1987) *Biochemistry 26*, 7042−7.
Leszyk, J., Collins, J. H., Leavis, P. C., & Tao, T. (1988) *Biochemistry 27*, 6983−7.
Morano, I., & Ruegg, J. C. (1991) *Pflugers. Arch. 418*, 333−7.
Moss, R. L. (1992) *Circ. Res. 70*, 865−84.
Moss, R. L., Giulian, G. G., & Greaser, M. L. (1985) *J. Gen. Physiol. 86*, 585−600.
Ohnishi, S., Maruyama, K., & Ebashi, S. (1975) *J. Biochem. 78*, 73−81.
Oton, J., Bucci, E., Steiner, R. F., Fronticelli, C., Franchi, D., Montemarano, J., & Martinez, A. (1981) *J. Biol. Chem. 256*, 7248−56.
Park, H. S., Gong, B. J., & Tao, T. (1994) *Biophys. J. 66*, 2062−5.
Parry, D. A., & Squire, J. M. (1973) *J. Mol. Biol. 75*, 33−55.
Potter, J. D. (1982) *Methods Enzymol. 85*, 241−63.
Potter, J. D., Seidel, J. C., Leavis, P., Lehrer, S. S., & Gergely, J. (1976) *J. Biol. Chem. 251*, 7551−6.
Satyshur, K. A., Pyzalska, D., Greaser, M., Rao, S. T., & Sundaralingam, M. (1994) *Acta Crystallogr. D50*, 40−9.
Siderer, Y., & Luz, Z. (1980) *J. Magn. Reson. 37*, 449−63.
Sundaralingam, M., Bergstrom, R., Strasburg, G., Rao, S. T., & Roychowdhury, P. (1985) *Science 227*, 945−8.
Szczesna, D., & Fajer, P. G. (1994) *Biophys. J. 66*, 188a.
Tao, T., Gowell, E., Strasburg, G. M., Gergely, J., & Leavis, P. C. (1989) *Biochemistry 28*, 5902−8.
Tao, T., Gong, B. J., & Leavis, P. C. (1990) *Science 247*, 1339−41.
Thomas, D. D., & Cooke, R. (1980) *Biophys. J. 32*, 891−906.
Wang, C. K., Liao, R., & Cheung, H. C. (1992) *Biochim. Biophys. Acta 1121*, 16−22.
Wang, C. K., Liao, R., & Cheung, H. C. (1993) *J. Biol. Chem. 268*, 14671−7.
Wang, C. L., & Gergely, J. (1986) *Eur. J. Biochem. 154*, 225−8.
Wang, Z., Gergely, J., & Tao, T. (1992) *Proc. Natl. Acad. Sci. U.S.A. 89*, 11814−7.
Zot, A. S., & Potter, J. D. (1989) *Biochemistry 28*, 6751−6.
Zou, G., & Phillips, G. N. (1994) *Biophys. J. 67*, 11−28.